Bangladesh J. Bot. **54**(3): 631-644, 2025 (September) Special DOI: https://doi.org/10.3329/bjb.v54i30.85186

ACIDIFICATION INDICES AND ORGANIC CARBON CHARACTERISTICS OF ACIDIC SOIL WITH DIFFERENT STRAW INCORPORATION RATES

ZHIFAN ZHANG[#], WENJIE BIAN[1#], JUN WAN, TAIBO LIANG[2], LI WANG[1], YI LI, KUI DING[1], BO WU[1], WENMIN CHEN, YU CHEN, HONGXU DONG[1*] AND MENGJIAO DING[2,3,4*]

Guizhou Provincial Tobacco Company Zunyi City Branch, Zunyi 563000, China

Key words: Acidic tobacco-growing soil, Straw incorporation rates, Characteristics of organic carbon, Acidification indices, Nutrient content

Abstract

This study analyzed the acidification indices and organic carbon differences of acidic tobacco-growing soils with different straw incorporation rates. The results showed that the Tengchong acidic tobacco-growing soil had low potential acidity and high base saturation. The long-term straw incorporation increased the organic matter year by year, but the soil pH in the tobacco growing season showed a decreasing trend. The ratio of humic acid to extractable humus (PQ), HA/FA value, E4 value, the rA value at 1630/cm in the infrared emission peak band, and the relative area after integration were significantly higher than those of the soils from Changning Jifei Town and Yongan Xiyang Town. The E4/E6 value, △logK value, and A2920/A1630 value of the soil collected from Tengchong were lower than those of soils from the other two areas. Thus, the soil from Tengchong had a high relative HA content in its humus composition and a complex organic carbon structure.

Introduction

As an important soil quality indicator, soil organic matter content affects the chemical composition and aroma-taste quality of tobacco leaves (Li *et al*. 2012, Ye *et al*. 2015). The carbon in soil organic matter is the organic carbon (SOC). The quantity and quality of SOC are closely related to maintaining and improving soil fertility, and their changes are closely related to tobacco yield, quality, style, and characteristics (He *et al*. 2014). Humus is a black or dark brown colloidal substance formed by the polymer organic compounds from soil organic matter decomposition and transformation under the action of microorganisms. Humus has a complex composition and a stable structure and can be divided into humin (HM), humic acid (HA), and fulvic acid (FA) according to the degree of dissolution in acid/base solutions (Stevenson 1994, Zhai *et al*. 2022). The contents and ratios of the three parts can characterize soil carbon stability and fertility. Research has shown that crop yield and quality are directly related to the composition characteristics of soil humus (Zhang *et al*. 2016, Nardi *et al*. 2021).

Different agricultural measures and ecological-climatic conditions significantly affect the water-soluble organic matter composition and HA functional group composition in the soil. Infrared spectroscopy can explain the functional group characteristics of soil organic matter and humus and reveal soil fertility status (MatěJková and Simon 2012, Wu *et al*. 2016). After determining the contents of organic carbon and each humus component in different acidic tobacco-growing soils, infrared spectroscopy was used to produce the infrared spectra of soil organic matter and analyze the functional group composition differences, thus, revealing the differences between the three acidic tobacco-growing soils from the perspective of functional group composition.

*Author for correspondence: <dhx9192@163.com>; <952156929@qq.com>. [1]China Tobacco Anhui Industrial Co. Ltd. Hefei, 230088, China. [2]Zhengzhou Tobacco Research Institute of CNTC, Zhengzhou 450001, China. [3]College of Tobacco Science of Guizhou University, Guiyang 550025, China. [4]Guizhou Provincial Key Laboratory for Tobacco Quality, College of Tobacco Science, Guizhou University, Guiyang 550025, China. [#]Zhifan Zhang and Wenjie Bian contributed equally to this work.

Soil humus composition and carbon functional group characteristics have always been hot topics for scholars worldwide (Zhou *et al*. 2021, Jia *et al*. 2024). Studying SOC pool composition characteristics and its driving factors is conducive to the quantitative evaluation of SOC pool quality and has important significance for accurately assessing the future evolution trend of SOC (Zou *et al.* 2013). The soil in different tobacco-growing regions in China is significantly different, as are the soil humus content, composition, properties, and carbon functional group characteristics. Previous research showed a significant negative correlation between humus carbon content and soil pH in the tobacco-growing area of southern Hunan (r = -0.356, p < 0.05) but an extremely significant positive correlation between humus carbon content and soil pH in the tobacco-growing area of central Henan (r = 0.471, p < 0.01) (Li *et al*. 2012). Therefore, soil pH affects the soil humus composition and has different relationships with the organic carbon compositions and structures in different regions. Acidic soil in different regions has different organic carbon compositions. The average soil organic matter content in the Tengchong tobacco-growing area is relatively high, and the average soil organic matter content in the Changning tobacco-growing area is relatively low (Li *et al*. 2019).

Straw which returned to the field cannot be decomposed in a short time. More undecomposed straw were accumulated in soil, causing humus composition and carbon structure of soil were changed. Tobacco-growing soil of Tengchong City had long-term straw returning to the field, but the soil pH was still decreasing with each passing year. Fujian Yongan, Yunnan Changning, and Yunnan Tengchong tobacco-growing areas suffer relatively severe soil acidification, making them three typical acidic tobacco-growing soil areas. According to the soil test for formula fertilization, Yongan has strong acidic (pH < 4.5), acidic (pH 4.5-5.5), and slightly acidic (pH 5.5-6.5) soils accounting for 5.2, 81.2, and 11.0%, respectively (Xu *et al.* 2002). Over two-thirds (67.6%) of the soil in the Tengchong tobacco-growing area is weakly acidic, and another 31.4% of the soil is strongly acidic. The soil acidification of the Changning tobacco-growing area is second to that in Tengchong (Li *et al*. 2017). To identify the organic carbon characteristics of tobacco-growing soil with straw returning, in this study, Changning soil without straw incorporation, Yongan soil with partial straw incorporation, and Tengchong soil with full straw incorporation were selected as the research subjects. The soil acidification indicators were determined by section sampling, and soil humus components and infrared spectra were determined with mixed cultivated layer soil samples. The humus composition, carbon functional group characteristics, and their relationships with soil factors were analyzed to clarify the differences in the carbon composition of acidic tobacco-growing soils in the three regions and the relationship with soil acidification.

Materials and methods

The types of acidic tobacco growing soil tested are shown in Table 1. For 5 consecutive years, the sampled soil plots in Changning had no straw incorporation, the sampled soil plots in Yongan had partial straw incorporation (rice roots), and the sampled soil plots in Tengchong had full rice and rape straw incorporation. Soil section sampling was conducted in February 2017 to determine the soil acidification indicators, where the soil samples were collected in layers according to the thickness, and each layer was sampled three times.

Table 1. Type of acidic tobacco-growing soil for experiment.

Sampling sites	Longitude and latitude	Altitude (m)	Cropping pattern	Soil type	Climate type
Yongan, Fujian	117.39 E,25.80 N	256.6	Tobacco rice rotation	Yellow paddy soil	Subtropical monsoon climate
Changning, Yunnan	99.42 E,24.68 N	1935.8	Dry farming	Yellow upland soil	Subtropical monsoon climate
Tengchong, Yunnan	98.63 E,25.42 N	1487.62	Tobacco rice rotation	Yellow paddy soil	Subtropical monsoon climate

The 5-point sampling method was employed near the excavated soil section, and mixed soil samples were collected from the 0-30 cm soil layer of seven field plots in each of the three areas for the analyses of relevant physical and chemical indicators, humus components, HA optical density, and Fourier transform infrared spectrum characteristics.

In addition, 200 kg mixed soil samples were collected from the cultivation layer in each area for the cultivation experiments and pot experiments. Determination of humus components/ total HA-FA carbon / HA carbon (Du and Gao 2006). Soil visible spectrum determination (Du and Gao 2006).

The concentration of the HA solution was adjusted to 0.136 mg/ml by dilution or concentration. The solution was zeroed on a GBC Cintra 1010 UV-Vis spectrophotometer with a reference of 0.05 mol/l sodium bicarbonate solution. The optical density E was measured with a 1 cm cuvette at the wavelengths of 726, 665, 655, 619, 600, 574, 533, 496, 465, and 400 nm of the visible spectrum. Absorption spectral curves were plotted using the 726, 655, 619, 574, 533, 496, and 465 optical density values, and the △logK value and E4/E6 value were calculated.

The △logK calculation method is as follows:

$\triangle \log K = \log A400 - \log A600$

The E4/E6 value calculation method is as follows:

$E4/E6 = A465/A665$

where A400, A460, A600, and A665 are the absorbance values at wavelengths 400, 465, 600, and 665 nm, respectively.

The SOC was determined with Fourier transform infrared transmission spectrometry: All samples were air-dried and screened through a 0.25 mm sieve before conducting the KBr pellet method. The soil sample and KBr were dried at 105°C for 12 hrs before being processed into pellets to prevent the hydroxyl groups in the excess moisture from interfering with the infrared spectrum (Calderón *et al.* 2011). An L104-IC electronic balance (0.0001 g) was used to measure 1 mg of the dried sample and 100 mg of dried KBr (spectrally pure, sample: KBr = 1 : 100), which were ground into a powder (particle size < 2 μm) in an agate mortar in an infrared dryer. The powder was thoroughly mixed in the agate mortar before being transferred and flattened into a pellet press, and a pressure of 10 t/cm^2 was applied and held for 1 min for pellet preparation. The pressed pellet (10 mm in diameter and 1 mm thick) was placed in the pellet clip and inserted into the infrared light path slot for infrared spectral transmission scanning, and the spectrum was recorded. The infrared spectrometer used here was a Nicolet IS10 Fourier transform-infrared spectrometer manufactured by Thermo Fisher in the United States, with a resolution of 4 cm^{-1} and a spectral scanning range of 4000-400 cm^{-1}. The number of scans was 32 times. Atmospheric and CO_2 background subtraction was performed during acquisition. Pure KBr pellet was used as the background, and the background spectrum was automatically deducted during scanning.

The following infrared spectra processing was conducted using Thermo Scientific OMNIC™ 8.2. After automatic baseline correction, 4000, 2000, and 860 cm^{-1} were used as the zero absorption points, and the straight lines passing the 3 points were used as the baselines for the integration of each absorption peak to calculate its relative correction area. Finally, the percentage of the area of each peak (the relative area of the absorption peak) is calculated and compared. By calculating the relative absorption intensity (rA), that is, rA of a certain band = the absorbance in this band/ the sum of absorbance of each peak band ×100 (Hernández-Montoya *et al.* 2012), the spectra of different treatments were compared.

In general, a mid-infrared spectrum is divided into two regions, 4000-1300 and 1300-600/ cm. The 4000-1300 cm^{-1} region used to characterize functional groups is also referred to as the group frequency region, functional group region, or characteristic region (Ndzelu *et al*. 2021). In contrast, the 1300–600 cm^{-1} region is called the fingerprint region. The spectral line changes in this region are more complex, and the molecular structure of the substance can be analyzed based on the subtle differences in absorption. Thus, this region can be used to distinguish between different compounds of similar structure. The study of the functional group characteristics of SOC and humus components is mainly concentrated in the functional group region.

Determination of soil physicochemical indicators (Du *et al*. 2006, Wu and Gao 2016). Moisture content: drying method (%); pH determination: water: soil = 2.5 : 1, potential method; Organic matter: potassium dichromate volumetric method (external heating method; g/kg); Total nitrogen: the Kjeldahl method (g/kg); Hydrolyzable nitrogen (alkaline hydrolysis nitrogen): alkaline hydrolysis diffusion method (mmol/kg); Available phosphorus: 0.5 M $NaHCO_3$ soaking extraction, molybdenum blue colorimetric method (mmol/kg); Rapidly available potassium: NH_4OAc soaking extraction, flame photometry (mmol/kg); Exchangeable calcium and Exchangeable magnesium: atomic absorption spectrophotometry (mmol/kg); Available sulfur: phosphate-acetic acid or calcium chloride extraction-barium sulfate turbidimetry (mmol/kg); Exchanging acids: potassium chloride exchange-neutralization titration (mmol/kg); Total exchangeable bases: neutralization titration (cmol/kg); Cation exchange capacity: ammonium acetate exchange method (cmol/kg); Base saturation (%) = total exchangeable bases/cation exchange capacity * 100.

The scanned spectral lines were analyzed and plotted using Fourier transform infrared spectroscopy software OMNIC and Origin 8.5. SPSS 18.0 was applied for data analysis. Infrared spectroscopy principal component analysis was performed using MATLAB.

Results and Discussion

Soil organic matter, total nitrogen, alkaline hydrolysis nitrogen, available phosphorus, and rapidly available potassium are important indicators of soil fertility (Liao *et al*. 2015). According to (Table 2), the soil nutrient contents of Tengchong Jietou Town at the sampling site were significantly higher than those of Yongan Xiyang Town and Changning Jifei Town, making it high-fertility tobacco-growing soil. By affecting the number and activity of soil microorganisms, soil pH greatly impacts soil nutrient availability and the growth and development of tobacco plants. Tobacco plant growth and development and its yield and quality are affected through the following two aspects. The first is to directly affect the root system growth, and the second is to affect the nutrient absorption of the tobacco plant by restricting the types, quantities, and effectiveness of plant nutrient elements in the soil. According to the information on soil tests for formula fertilization in the three tobacco-growing areas in 2017, all soil samples have strong acidity (pH < 5.5).

Table 2. Analysis of physical and chemical properties of soil in three typical acidic tobacco-growing areas (n=7, p ≤0.05).

Sampling sites	pH	Organic matter g/kg	Total nitrogen g/kg	Alkaline hydrolysis nitrogen mg/kg	Available phosphorus mg/kg	Available potassium mg/kg
Yongan	5.12 ± 0.06a	23.67 ± 0.96c	0.71 ± 0.02c	70.06 ± 1.41b	14.56 ± 0.55b	287.00 ± 6.66c
Changning	4.48 ± 0.06b	29.83 ± 0.47b	0.87 ± 0.02b	73.18 ± 1.23b	28.77 ± 0.78a	362.18 ± 6.42b
Tengchong	5.22 ± 0.06a	61.85 ± 1.22a	1.54 ± 0.07a	166.32 ± 6.18a	30.84 ± 0.89a	614.04 ± 3.81a

From Baoshan tobacco-growing areas in Yunnan Province and Sanming tobacco-growing areas in Fujian Province at the same latitude, Jietou Town in Tengchong City, Jifei Town in Changning County, and Xianyang Town in Yong'an City affected by solid acidification were selected for sampling and analysis of typical acidic soil slopes (0-100 cm). As can be seen from Table 3, Baoshan tobacco-growing areas include two ecological zones separated by the Longchuan River, with Tengchong City to its east and Changning County to the west. The acidification indices of the 0-100 cm tobacco planting soils pronouncedly differ in these two areas. The organic matter, exchangeable Ca, exchangeable Mg, total exchangeable base, cation exchange capacity, and base saturation in the acidic soils in Jietou Town are significantly higher than those in Jifei Town, and these values are in line with the definition of high fertility soils in soil science. Conversely, Jifei soil has significantly higher contents of available sulfur and exchangeable acidity than Jietou soil. Compared to the acidic soil in Jietou, the soil in Xiyang Town, Yongan City exhibits no significant differences in soil pH and a significantly high content of exchangeable acidity. Despite low potential acid content and high base saturation in the acidic tobacco growing soil in Tengchong, the pH values during the flue-cured tobacco growing season decrease year by year, largely affecting the growth and quality improvement of flue-cured tobacco. For the low cation exchange capacity, exchangeable Ca, and exchangeable Mg in the acidic soils in Xiyang and Jifei towns, the application of alkaline mineral fertilizers (such as lime) can greatly improve soil acidification. However, the long-term improvement effect on the acidic tobacco-growing soil in Jietou Town, Tengchong, is not obvious (Dou *et al.* 2007). The acidification indices of different soil layers were analyzed, and a slight difference was seen in the depth of 0-60 cm. When increasing the depth to 60-100 cm, these indices changed greatly, further increasing the difficulty of improving acidified soil in tobacco-growing areas in later stages.

Table 3. Analysis of acidification index of soil in three typical acidic tobacco-growing areas (n=3).

Soil depth (cm)	pH	Organic matter	Exchangeable calcium (Ca)	Exchangeable magnesium (Mg)	Available sulfur (S)	Total exchangeable base	Cation exchange capacity	Base saturation	Exchangeable acidity
		g/kg	mg/kg	mg/kg	mg/kg	cmol/kg	cmol/kg	%	mmol/kg
Yongan									
0-15	5.15	24.90	401.6	19.28	17.15	13.31	16.29	81.71	18.05
15-30	4.95	20.08	389.6	12.97	11.80	12.56	14.34	87.59	17.65
30-60	4.88	16.98	356.4	11.76	8.63	12.11	13.89	87.19	15.32
60-100	4.65	12.21	357.8	9.27	8.32	13.16	14.91	88.26	13.69
Changning									
0-15	3.97	12.29	327.6	46.26	23.55	8.76	10.98	79.81	22.07
15-30	3.88	10.64	302.4	53.82	29.71	7.85	10.12	77.55	22.24
30-60	3.84	7.13	281.4	64.42	9.96	9.40	11.21	83.82	18.02
60-100	4.21	4.28	331.8	90.25	5.25	10.21	11.62	87.87	13.97
Tengchong									
0-15	5.20	35.03	1520	88.85	8.52	21.97	22.26	98.68	2.78
15-30	5.08	44.28	1402	86.9	7.97	28.25	28.50	99.13	2.30
30-60	5.07	28.30	1247	81.82	6.88	17.40	17.74	98.09	2.67
60-100	4.80	18.75	869	65.07	12.50	15.00	15.33	97.86	3.16

Comparative results of soil humic components in tobacco-growing areas are shown in Table 4. The carbon content of humus, HA, fulic acid, and HM in the study area of Jietou is significantly higher than that of Jifei and Xiyang. In addition, the carbon content of each humic component in Jifei is significantly higher than that in Xiyang. PQ or HA/FA are typically used to describe the composition and complexity of soil humus. The changes in PQ and HA/FA values allow clarification of the relative rate of formation of humic and FAs in different soils or under various cultivation conditions and the transformation relationships among humic components (Dou and

Jiang 1988, Dou *et al*. 2007), and both indicators were employed for describing the degree of humification. As can be seen from Table 4, the PQ and HA/FA in the Jietou soil are significantly higher than those in the other two soils, indicating that the sampled humus has higher HA content and more complex structures.

Table 4. Analysis of humus components of soil in three typical acidic tobacco-growing areas (n=7, p ≤ 0.05).

Sampling sites	Humus carbon g/kg	HA+FA carbon g/kg	HA carbon g/kg	FA carbon g/kg	HM carbon g/kg	HA/FA	PQ
Yongan	13.73 ± 0.56c	4.20 ± 0.06c	1.51 ± 0.11c	2.69 ± 0.09c	9.53 ± 0.56c	0.57 ± 0.07b	35.89 ± 2.45b
Changning	17.3 ± 0.27b	5.65 ± 0.11b	2.17 ± 0.15b	3.48 ± 0.14b	11.65 ± 0.26b	0.63 ± 0.06b	38.29 ± 2.42b
Tengchong	35.88 ± 0.71a	12.04 ± 0.22a	5.56 ± 0.24a	6.48 ± 0.28a	23.84 ± 0.78a	0.87 ± 0.07a	46.17 ± 1.92a

The content and proportion of soil humic components can reflect the complexity of humus. The optical properties of HA involved in soil humic components in the visible light band fundamentally explain the degrees of aromatization and condensation as well as the chemical stability of the acid. Such optical properties refer to the absorbance value of dissolved humus in the visible or ultraviolet region, such as E4, E4/E6, and tone coefficient (△logK) values, and are mainly used to estimate the complexity or humification of humus molecules (Bernard *et al.* 2022).

E4 is an indicator of the complexity degree of soil humus, and it is significantly positively correlated with the soil aromatization degree (Liu *et al*. 2012). Specifically, a higher E4 value indicates a larger complexity of molecules, more aromatic groups, and greater condensation. In contrast, a simpler structure for HA means less aromaticity, more aliphatic side chains, and fewer optical density (Li *et al.* 2018). Table 5 demonstrates that the E4 value of the Jietou soil is relatively high, indicating the great complexity of soil humus. E4/E6 is the ratio of the optical density of HA alkaline solution at 465 and 665 nm, and a smaller E4/E6 value corresponds to higher molecular complexity, more aromatic nuclei, and greater condensation. Conversely, less complexity indicates smaller aromatization and greater aliphatic bonds, corresponding to a larger E4/E6 value. As shown in Table 5, the E4/E6 values in the Jietou soil are the lowest among all samples, indicating a relatively high aromatization and humification. In contrast, soils from Jifei and Xiyang display relatively small aromatic ring condensation and simple structure. The △logK can reflect the complexity of the molecular structure of soil humus; a higher △logK value is consistent with a simpler molecular structure (Ren *et al*. 2024). In addition, a higher △logK of HA means higher contents of methoxy and alcohol hydroxyl groups, lower contents of carboxyl, carbonyl, and phenol hydroxyl groups, and weaker oxidation (Lu *et al*. 2015). The tone coefficients in Xiyang and Jifei soils were higher than those in Jietou soil, indicating the simple molecular structure of soil humus in the former two towns. To conclude, △logK, E4/E6, and E4 values all indicated that the soil in Jietou had a high degree of secondary humification.

Table 5. Analysis of humic acid optical properties of soil in three typical acidic tobacco-growing areas (n=7, p ≤0.05).

Sampling sites	400 nm	600nm	E4/E6	△logK
Yongan	0.1000	0.0201	5.1672	0.6965
Changning	0.1287	0.0259	4.4441	0.6965
Tengchong	0.1376	0.0315	4.2461	0.6402

The optical density curve was plotted by setting the carbon content of the HA solution to 0.136 g/l and measuring the absorbance values at different wavelengths (Fig. 1). When the absolute value of slope (steepness) is large, the molecular complexity is low (Lu *et al*. 2015). Accordingly, the steepness of the optical density curve shows that the slope in Jifei and Xiyang towns is greater than that in Jietou Town, indicating lower complexity of HA molecules in the former two soils.

E465 (l/g/cm) refers to the absorbance value of HA in the visible region at a given concentration, allowing for reflection of the degree of condensation and molecular complexity of HA (Sharaf *et al*. 2021). Figure 1 shows the different absorbance values of HA in various acidic tobacco-growing soils, following an E465 order of Jietou > Jifei > Xiyang, proving the high complexity in Tengchong.

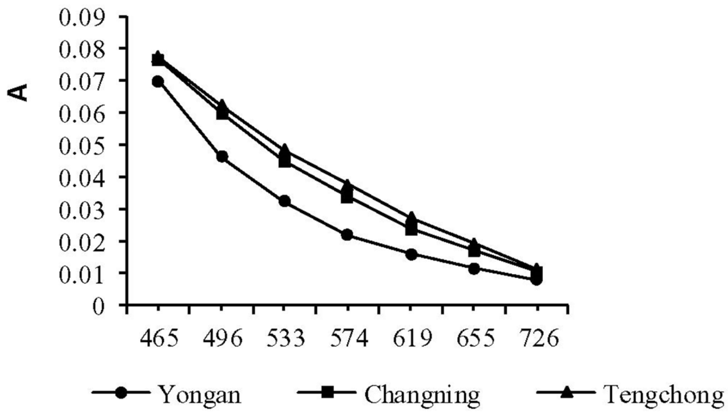

Fig. 1. Analysis of optical density curves of soil in three typical acidic tobacco-growing areas (n=7, p ≤0.05).

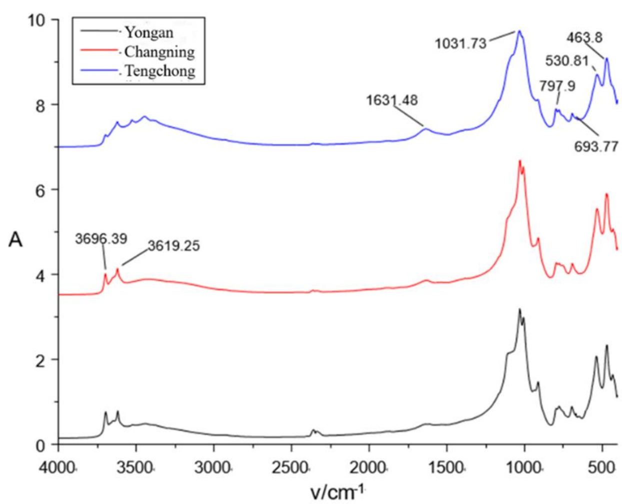

Fig. 2. Fourier infrared absorption spectroscopy of soil in three typical acidic tobacco-growing areas (4000-400/cm).

Fourier transform infrared spectroscopy was deployed to fully reveal the relationship between the molecular structure of SOC and its acidification indices. (Figs 2 and 3) demonstrate that the characteristic infrared spectral peaks of acidic tobacco-growing soils are consistent despite slight variations. The main characteristic peaks in the three areas are at 3696, 3648, 3620, 3525, 3443, 3394, 3375, 2919, 2847, 1630, 1107, 1029, 1010, 913, 797, 775, 695, 536, and 473 cm^{-1} (Table 6), indicating consistent carbon skeleton structures in tobacco-growing soils after long-term tillage

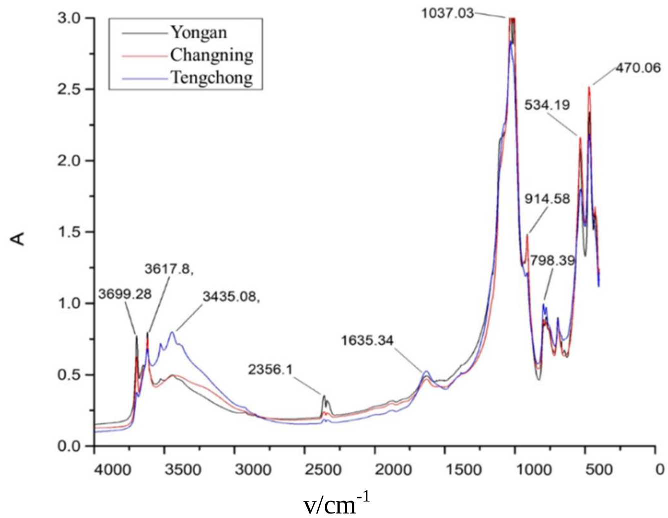

Fig. 3. Fourier infrared absorption spectroscopy of soil in three typical acidic tobacco-growing areas (4000-400cm^{-1}).

Table 6. Analysis of infrared spectrum absorption peak and relative absorption intensity of soil in three typical acidic tobacco-gegrowing areas (n=7, p ≤0.05).

Wave number/cm^{-1}	Mode of blade vibration	Relative absorption strength (rA)		
		Yongan	Changning	Tengchong
3696	-OH stretching vibration	2.44	1.66	1.28
3648	-OH stretching vibration	1.78	1.48	1.76
3620- 913	-OH deformation vibration	2.69	2.40	2.39
3525	-OH stretching vibration	2.13	2.15	2.81
3443	-OH deformation vibration or N-Hstretching vibration	2.52	2.81	3.30
3394	Phenolics -OH stretching vibration，N-H stretching vibration	2.28	2.60	2.87
3375	Phenolics -OH stretching vibration，N-H stretching vibration	2.15	2.42	2.74
2925	C-H of -CH_2 antisymmetric stretching vibration	0.94	0.80	0.89
2847	C-H of -CH_2symmetrical stretching vibration	0.70	0.46	0.86
2361		0.66	0.61	0.71
2343		0.65	0.55	0.71
1869	Cyclic anhydride C= antisymmetric stretching vibration	1.07	0.83	1.11
1630	C=C stretching vibration of aromatic structure, deformation vibration of hydrogen bond formation of water molecules, C=O stretching vibration with hydrogen bond, antisymmetric stretching vibration of -COO- in carboxylate carboxylate group, C=O stretching vibration of lignin connected to aromatic ring, N-H stretching vibration of amino acid	2.10	1.76	2.54
1107	The stretching vibration of C-O in carbohydrates and the absorption peaks formed by silicate minerals (Si-O stretching vibration) and sulfate in inorganic compounds	9.97	9.15	9.23
1029		13.89	14.68	13.45
1010		19.43	20.16	18.36
913	C-H out-of-plane rocking vibration in olefin	5.65	5.27	5.06
797	Si-O-Si stretching vibration	3.82	3.91	4.42
775	C-H bending vibration on aromatic ring	4.19	3.81	4.31
695	Olefin cis-= C-H out-of-plane bending vibration	3.47	3.22	3.73
536	Si-O-Mg、Si-O-Al bending vibration	8.13	8.32	7.74
473	Si-O-Si bending vibration	9.33	10.94	9.73
A2920/A1630		0.46	0.47	0.31

measures. The three soils have three main absorption zones, respectively, at 3000-3800, 1300-1800, and 500-1200 cm^{-1}. Changning and Yong'an tobacco-growing soils are acidic with low organic matter content, explaining the consistent absorption peaks as well as the similar absorbance values in the 500-1200 cm^{-1} fingerprint area. The infrared spectral absorption peaks of acidic tobacco-growing soils in the three sites have different resonance intensities at various wavelengths (Table 6). At 3394 and 3375 cm^{-1}, the absorption peaks belong to the stretching vibration of the hydroxyl group of phenolic compounds; in addition, the soil signals in Jietou, Tengchong are higher than other soils at these absorption regions, indicating that the -OH group content of phenolic compounds is high. The peaks at 2920 and 2847 cm^{-1} correspond to asymmetric and symmetric stretching vibrations of aliphatic -CH_2 and the corresponding soil signals in Jietou and Xiyang towns are higher than those in Jifei Town. The potential reason is that Jifei soil has relatively low organic carbon and activated carbon component content. The peaks within 1630/cm are attributed to the aromatic C=C stretching vibration, the deformation vibration of hydrogen bonds formed by water molecules, the C=O stretching vibration with hydrogen bonds, the antisymmetric stretching vibration of -COO- in the organic carboxylate group, the C=O stretching vibration bonded to the aromatic ring in lignin or the N-H stretching vibration in amino acids (MatěJková and Šimon 2012, Wu *et al.* 2016). The absorption peak (775/cm) in Jietou soil is the highest in all soils, corresponding to the C-H bending vibration on the aromatic ring, indicating that the soil structure in the Jietou study site is complex. The absorption peaks at 1107, 1029, and 1010/cm correspond to the stretching vibrations of C-O in carbohydrates and are formed by silicate minerals (Si-O stretching vibration) and sulfates of inorganic compounds, and the highest ones are detected in Jifei Town. As seen from A2920/A1630 values, Tengchong has a relatively high content of inert carbon functional groups.

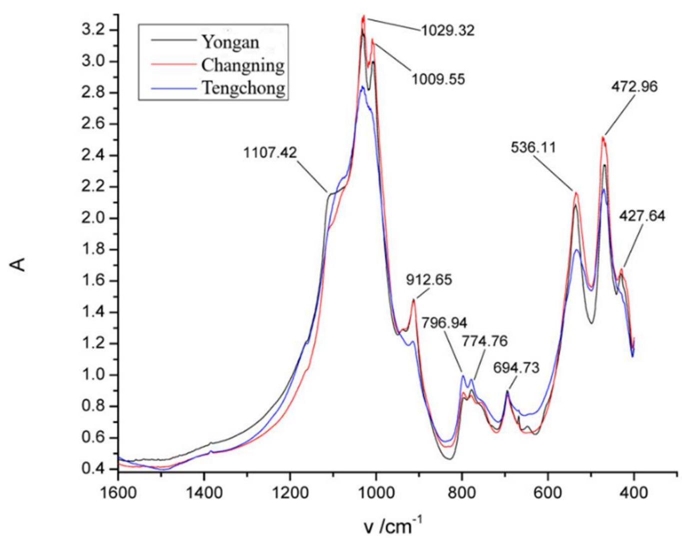

Fig. 4. Fourier infrared absorption spectroscopy of soil in three typical acidic tobacco-growing areas (1600-400 cm^{-1}).

In the case of the absorption peak at 2920 cm^{-1}, the Jietou soil has a higher absorption intensity than the Jifei soil, and the relative area obtained by integral can be ignored. For this reason, only active groups at 1110-1000 cm^{-1} are considered. According to Table 7 and Figs 4-6) unstable functional groups include alcoholphenol free-OH, polysaccharide C-O, and aliphatic-CH, and stable functional group structures are aromatic C=O and C=C. Jifei soil has relatively few stable structures, and increased structures readily decomposed, simplifying the organic matter structure and reducing the carbon content. Notably, the effects of adding lime and mineral potash fertilizer during soil acidification are pronounced, and the soil pH and the content of alkaline cations such as Ca and Mg can be quickly raised. Conversely, the carbon structure of Tengchong soil tends to be complex, increasing stable carbon structures. The regional rainfall is high, and the inert carbon component is destructive to the storage of alkaline cations. In this sense, alkaline fertilizer alone cannot effectively improve soil acidification. To fundamentally overcome the problem of soil acidification in the Tengchong tobacco-growing areas, the carbon components and structure of the high organic matter soil in Tengchong need to be adjusted to achieve the effects of fertilizer preservation and sequestration of exchangeable cations.

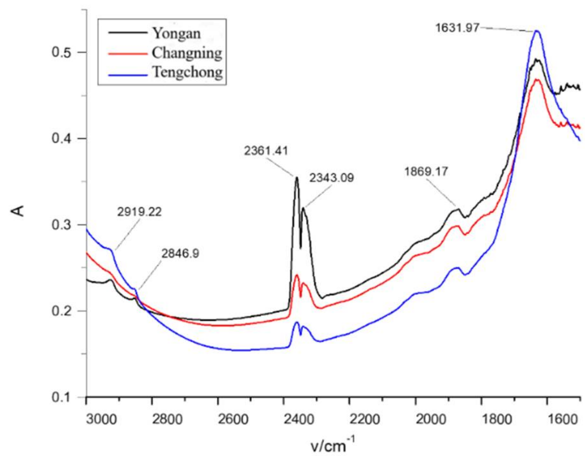

Fig. 5. Fourier infrared absorption spectroscopy of soil in three typical acidic tobacco-growing areas (3000-1500cm^{-1}).

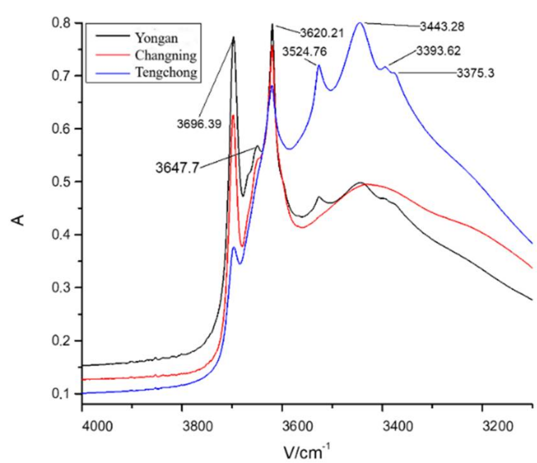

Fig. 6. Fourier infrared absorption spectroscopy of soil in three typical acidic tobacco-growing areas (4000-3100 cm^{-1}).

Figure 7 indicates that the acidic soils can be further divided, with Jifei and Xiyang soils as a group based on the presence of organic carbon structure and the soil in Jietou Town as the other category, suggesting the various carbon structures in the two groups of soils.

Table 7. Corrected area of infrared spectral absorption peaks of soil in three typical acidic tobacco-growing areas.

Absorption peak wave number/cm	Affiliation	Corrected area
1107、1029、1010	C-O stretching vibration of polysaccharides	Changning (11.83%)>Yongan (11.00%)>Tengchong (7.40%)
1630	C=C，Phenol aromatic ring stretching vibration (Aromatic C=C)	Changning (0.91%)<Yongan (1.10%)<Tengchong (3.12%)

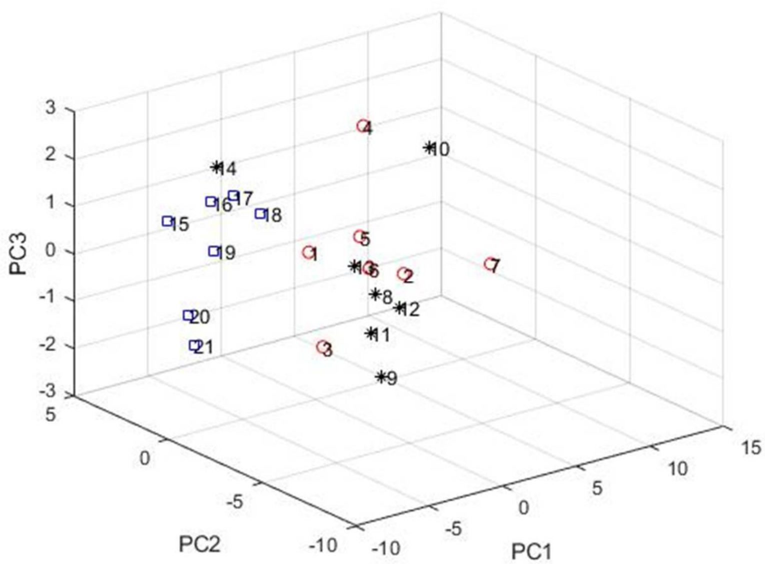

Fig. 7. Principal component analysis of fourier infrared absorption spectroscopy of soil in three typical acidic tobacco-growing areas.

The organic matter, exchangeable Ca, exchangeable Mg, total exchangeable base, cation exchange capacity, and base saturation of the acidic soils in Jietou Town, Tengchong City, are significantly higher than those in Jifei Town, Changning County, and these values are all in line with the traditional definition of high-fertility soil. This is consistent with previous research results demonstrating that the proportion of soils with moderate to rich content of organic matter, rapidly available nitrogen, and rapidly available phosphorus in Tengchong City is higher than in other counties (Xu *et al*. 2008). The exchangeable acidity content in the Jifei and Xiyang soils is significantly higher than in the Jietou soils. Tengchong acidic tobacco planting soil has a low potential acid content and high base saturation; however, the soil pH during flue-cured tobacco growing season decreases yearly. Straw incorporation in the regional tobacco-growing soils improves organic matter, yet no significant effect is observed on improving soil acidification. Based on the above analysis, identifying the differences in carbon structure between acid tobacco growing soils in Tengchong as well as Changning and Yong'an can further explain the increased organic matter content fertility and the poor improvement of the flue-cured tobacco quality following straw incorporation.

The soil carbon characteristics analysis showed that PQ and HA/FA in Jietou were significantly higher than those in Jifei and Xiyang, indicating that the Tengchong soil had a high relative HA content and a complex structure; the E4 value of the Jietou soil was relatively high, and its E4/E6 value was lower than that of the other two towns. Furthermore, the smaller △ logK value of the soil in Jietou town indicated high HA aromatization and humification. The complex humic components in Tengchong soil can also be proved by the optical density curve and E465 values. Fourier transform infrared spectral analysis demonstrated that the peaks within 1630 cm^{-1} are attributed to the aromatic C=C stretching vibration, with the highest absorption peak and the largest relative area after integration in Jietou. In this range, unstable functional groups include alcoholphenol free -OH, polysaccharide C-O, and aliphatic -CH, and the stable functional group structures involve aromatic C=O and C=C. For this wave range, the relative area is the smallest, further indicating that the carbon structure of Tengchong soil tends to be complex. The reason for the complex humic components, the maximum proportion of HA, and the high aromatization in Jietou soil may be that the long-term straw incorporation led to an elevated proportion of newly formed HAs and the "rejuvenation" in composition, that is, the newly formed HA contains more lignin components, which contained in soil litterfall can hinder the decomposition of organic carbon components (Zhang *et al*. 2019). This is consistent with previous findings that applying corn stalk could increase the shoulder absorption intensity at 285 nm, and absorption enhanced with increasing corn stalk (Xu *et al*. 2008). To address the soil acidification problem in Tengchong, attempts can be made to accelerate the decomposition of lignin components through agricultural measures and improve the humus and carbon contents in soils.

Acknowledgements

The work was supported by the National Natural Science Foundation of China (Grant No. 42467007), Guizhou Science and Technology Partnership Initiative, Basic Research Grant [2024] Youth 177, the Science and Technology Project of Zunyi Tobacco Company (Grant No. 2022XM06), the Technical Service Project of Anhui Tobacco Base Unit (Grant No. 2024340000340003), the Key Program for Science and Technology of CNTC (No.110202402016), the Science and Technology Program of Guizhou Provincial Branch of the CNTC (No. 2024520000240022, 2023520000240241), the Program of Hubei Xinye Tobacco Slice Development Co., Ltd (No. N2024420114360067). Guizhou Provincial Key Laboratory Construction Project for Tobacco Quality Improvement and Efficiency Enhancement Guizhou Science and Technology Innovation Platform ZSYS (2025) 028.

References

Bernard L, Basile DI, Derrien D, Fanin N, Fontaine S, Guenet B, Karimi B, Marsden C and Maron P 2022. Advancing the mechanistic understanding of the priming effect on soil organic matter mineralisation. Funct. Ecol. **36**(6): 1355-1377.

Calderón FJ, Reeves JB, Collins HP and Paul E 2011. Chemical differences in soil organic matter fractions determined by diffuse-reflectance mid-infrared spectroscopy. Soil Sci. Soc. Amer. J. **75**(2): 568-579.

Dou S, Yu SQ and Zhang JJ 2007. Effects of carbon dioxide concentration on humus formation in corn stalk decomposition. Acta Pedolog. Sin. **44**(3): 458-466.

Dou S and Jiang Y 1988. Effect of application of organic materials on the properties of humic substances in organo-mineral complexes of soils II effect of organic materials on the humus composition and optical characteristics of humic acids in organo-mineral complexes. Acta Pedolog. Sin. **3**: 252-261.

Du S and Gao XZ 2006. Technical specifications for soil analysis (second edition). Chinese Agricultural Press, China.

Hernández-Montoya V, Alvarez LH, Montes-Morán MA and Cervantes F 2012. Reduction of quinone and non-quinone redox functional groups in different humic acid samples by *Geobacter sulfurreducens*. Geoderma **183**: 25-31.

He YT, Wang CQ, Li B, Wang WQ, Li B, Xiang JY and Lei B 2014. Effect of humic acid application on the yield and quality of flue-cured tobacco. J. Agricul. Sci. **6**(11): 8.

Jia GT, Chen XL, Wang GF and Yang XL 2024. Theory and practice of developing specialty and high-quality tobacco leaves in west Henan Province of China. Cayley nielson press, inc.

Li CL, Xu JB, He YQ, Liu YL and Fan JB 2012 Dynamic relationship between biologically active soil organic carbon and aggregate stability in long-term organically fertilized soils. Pedosphere **22**(5): 616-622.

Li HP, Ding MJ, Zhang FM, Liu H, Duan ZC, Zhou JH, Fan W, Xiao ZX and Zhang Y 2017. The effect of different new potassium-rich soil conditioners on potassium applying characteristics of soils and tobacco quality. Chinese Tobac. Sci. **38**(4): 64-69.

Li J, Wen YC, Li XH, Li YT, Yang XD, Lin ZA, Song ZZ, Cooper JM and Zhao BQ 2018. Soil labile organic carbon fractions and soil organic carbon stocks as affected by long-term organic and mineral fertilization regimes in the North China Plain. Soil Res. Till. **175**: 281-290.

Li JY, Deng XP, Yang K, Li DF, Yang YH and Jin Y 2012. Effect of organic fertilizer on soil physicochemical property in tobacco field. Soil Fertil. Sci. China **34**: 12-16.

Li XD, Wu B, Zhang Q, Xu DP, Liu YQ, Ma FJ, Gu QB and Li FS 2019. Mechanisms on the impacts of humic acids on persulfate/Fe2+-based groundwater remediation. Chem. Eng. J. **378**: 122142.

Liao D, Yu DS, Zhao YC, Wang N, Zhang HD, Pan JJ and Shi XZ 2015. Composition of organic carbon in paddy soil in typical area of Chengdu and its influencing factors. Acta Pedolog. Sin. **52**(3): 517-527.

Liu Y, Li DY and Cheng ZH 2012. Main nutrient status of tobacco-planting soil in Baoji and fertilization suggestions. Acta Agricul. Jiangxi **24**(08): 18-21.

Lu XK, Mao QG, Mo JM, Gilliam FS, Zhou GY, Luo YQ, Zhang W and Huang J 2015. Divergent responses of soil buffering capacity to long-term N deposition in three typical tropical forests with different land-use history. Environ. Sci. Technol. **49**(7): 4072-4080.

MatěJková Š and Šimon T 2012. Application of FTIR spectroscopy for evaluationof hydrophobic/hydrophilic organic components in arable soil. Plant Soil Environ. **58**(4): 192-195.

Nardi S, Schiavon M and Francioso O 2021. Chemical structure and biological activity of humic substances define their role as plant growth promoters. Molecules **26**(8): 2256.

Ndzelu BS, Dou S, Zhang XW, Zhang YF, Ma R and Liu X 2021. Tillage effects on humus composition and humic acid structural characteristics in soil aggregate-size fractions. Soil Res. Till. **213**: 105090.

Ren K, Gu KY, Song WF, Su JE, Yang ZM, Chen Y, Hu BB, He CG, Wang LC and Zou CM 2024. Legacy effects of preceding crops improve flue-cured tobacco productivity in southwest China by optimizing soil structure, nutrients, and microbial interactions. Plant Soil 504: 247-269.

Sharaf A, Wu JG, Fan W, Hu J, Opoku-Kwanowaa Y, El-Rahim MA and Moussa AA 2021. Changes in soil humic acid composition after nine years of repeated application of organic wastes in black soil: a study using solid-state FT-IR and (13 C-NMR) analysis. Polish J. Environ. Stud. **30**(6).

Stevenson FJ 1994. Humus chemistry: genesis, composition, reactions. John Wiley and Sons.

Wu JP, Liang GH, Hui DF, Deng Q, Xiong X, Qiu QY, Liu JX, Chu GW, Zhou GY and Zhang DQ 2016. Prolonged acid rain facilitates soil organic carbon accumulation in a mature forest in Southern China. Sci. Total Environ. **544**: 94-102.

Wu M, Li ZP, Feng YZ, Chen RR, Jiang CY and Liu M 2016. Dynamic differences of organic carbon mineralization in different types of paddy soil under long-term located fertilization. Sci. Agricul. Sin. **49**: 1705-1714.

Xu CY, Shen QR and Ran W 2002. Effects of zero-tillage and application of manure on soil microbial biomass C, N, and P after sixteen years of cropping. Acta Pedolog. Sin. **39**: 89-95.

Xu ZC, Li YY, Xiao HQ and Wang L 2008. Evaluation of ecological factors and flue-cured tobacco quality in tobacco-growing areas in southern Hunan, China. Chinese J. Plant Ecol. **32**(1): 226.

Ye XF, Zhou HJ, Li ZP, Yu XN, Niu YD, Li XF, Guan SS, Zong SJ and Zhang S 2015. Effects of biochar types on carbon pool in tobacco-planting soil and quality of flue-cured tobacco leaves. Acta Tabac. Sin. **21**: 33-41.

Zhai X, Zhang L, Wu RF, Wang M, Liu YX, Lian JP, Munir MAM, Chen D, Liu L and Yang XE 2022. Molecular composition of soil organic matter (SOM) regulate qualities of tobacco leaves. Sci. Rep. **12**(1): 15317.

Zhang G, Dou S, Xie ZB, Zhong SL, Yang XY, Zhou X and Yin XB 2016. Effect of biochar application on composition of soil humus and structural characteristics of humic acid. Acta Sci. Circumst. **36**: 614-620.

Zhang JM, An TT, Chi FQ, Wei D, Zhou BK, Hao XY, Jin L and Wang JK 2019. Evolution over years of structural characteristics of humic acids in Black Soil as a function of various fertilization treatments. J. Soils Sedim. **19**: 1959-1969.

Zhou H, He H, Xiao M and He ZJ 2021. Composition of humus in forest soils of Yunnan province, China and its influencing factors. Acta Pedolog. Sin. **58**: 1008-1017.

Zou HT, Guan S, Ling Y, Fan QF, Zhang YL and Huang Y 2013. Effect of different straw return years on humus composition of soil. Chinese J. Soil Sci. **44**: 1398-1402.

(Manuscript received on 16 May 2025; revised on 14 October 2025)